Pharm Res (2010) 27:1999–2007
DOI 10.1007/s11095-010-0204-9

RESEARCH PAPER

An Improved Nonlinear Model Describing the Hepatic Pharmacokinetics of Digoxin: Evidence for Two Functionally Different Uptake Systems and Saturable Binding

Michael Weiss • Peng Li • Michael S. Roberts

Received: 6 April 2010 / Accepted: 22 June 2010 / Published online: 13 July 2010

ABSTRACT

Purpose To develop a semi-distributed liver model for the evaluation of saturable sinusoidal uptake and binding kinetics of the Oatp1a4 substrate digoxin.

Methods In the perfused rat liver, two successive digoxin doses of 42 and 125 μg were administered, and the outflow concentration was determined by LC/MS/MS. [^{14}C]-sucrose was used as vascular reference. The data were analyzed simultaneously by a population approach using sucrose to determine the sinusoidal mixing of digoxin.

Results The results suggest the existence of a high-affinity, low-capacity system, and a low-affinity, high-capacity system for sinusoidal uptake with apparent Michaelis constants (K_M) of 0.24 and 332 μg/ml, respectively. Incorporation of saturable sinusoidal binding of digoxin considerably improved the fit, and the parameter estimates were consistent with those of binding to hepatic Na,K-ATPase. Simpler models that neglect the concentration gradient in flow direction failed to describe the outflow data in the high dose range.

Conclusion The semi-distributed liver model with saturable uptake should be useful for a functional characterization of transporters in the *in situ* rat liver.

KEY WORDS digoxin · drug transporters · hepatic sodium pump · hepatic uptake · kinetic model · Oatp1a4 · rat liver

M. Weiss (✉)
Section of Pharmacokinetics, Department of Pharmacology
Martin Luther University Halle-Wittenberg
06097 Halle, Germany
e-mail: michael.weiss@medizin.uni-halle.de

P. Li · M. S. Roberts
Department of Medicine, Princess Alexandra Hospital
University of Queensland
Woolloongabba, Queensland, Australia

INTRODUCTION

Given the importance of hepatic drug clearance, a quantitative understanding of the role of transporters expressed in the liver becomes increasingly relevant since in addition to metabolism, elimination of drugs can be dependent on hepatic transport processes (e.g., 1,2). A critical point in the evaluation of the function of hepatic uptake transporters has been the need of a suitable mathematical model of the liver. Such models can be classified as lumped parameter and distributed models. Distributed models have the advantage of being more realistic than lumped parameter models, which assume instantaneous mixing within compartments. However, due to the inherent assumption of system linearity, distributed models cannot be used if saturable processes are involved, e.g., for the estimation of the transporter Michaelis-Menten parameters, K_M and V_{max}. Recently, we described the use of a compartmental liver model to analyze sinusoidal uptake kinetics of the selective Oatp1a4 (formerly Oatp2) substrate digoxin in perfused rat liver (3). The goal of this study was to determine whether the assumption of a well-mixed vascular space and the limited dose range could have influenced parameter estimates. The second goal to be addressed was the effect of binding of digoxin to hepatic Na,K-ATPase, located at the basolateral membrane. Although it is well established that rat hepatocytes express the α_1-isoform of Na,K-ATPase (4,5), the effect of saturable digoxin binding has not been considered in previous models of hepatic digoxin processing (3,6,7). A possible influence of hepatic binding on saturable processes occurring in the liver was already pointed out by Rubin and Tozer (8); however, this mechanism has received less attention.

To accomplish these goals, we first incorporated saturable processes for both sinusoidal binding and uptake into a

semi-distributed liver model that accounts for the concentration gradient in flow direction (between the portal and central veins) by dividing the system into smaller groups of compartments (9). Second, isolated-perfused rat liver experiments were performed with higher doses of digoxin than used in the first study (3). Since for two saturable uptake mechanisms (double Michaelis-Menten equation) in addition to saturable binding, the fitting problem is extremely ill-conditioned, unique and stable parameter estimates are sought by incorporating prior information using a population approach (10). In fitting the outflow data of all single-pass perfused livers simultaneously, information from the entire population instead of only one liver is put to use (e.g., 11).

Our results emphasize the role of the modeling process and suggest that a high- and a low-affinity component are involved in hepatic uptake of digoxin. Such atypical transport mechanisms characterized by multiple binding sites have been found previously in several transporters including Oatps (eg, 12,13). However, a large range of substrate concentrations must be used to detect both the high- and low-affinity binding sites.

MATERIALS AND METHODS

Chemicals

Digoxin was purchased from Sigma Aldrich (St. Louis, MO); [U-^{14}C]sucrose was purchased from New England Nuclear (Boston, MA). Digoxin was dissolved in 70% ethanol solution and diluted with MOPs buffer. The final concentration of ethanol in perfusate was less than 0.5%. All other chemicals and solvents were of the highest grade available.

In Situ Perfusion of the Isolated Rat Liver

Perfusion of the isolated rat liver used in this study was performed as described elsewhere (14). Briefly, male Wistar rats, weighing 200–250 g were anaesthetized using an intraperitoneal injection of xylazine/ketamine (10/80 mg·kg^{-1}). The laparatomized rats were heparinized with 200 units heparin injected into the inferior vena cava. The bile duct and the portal vein were cannulated (PE-10, Clay Adams, Franklin Lakes, NJ) and using an intravenous 16-gauge catheter, respectively. The liver was then perfused with MOPS [3-(N-morpholino-)propanesulfonic acid]-buffer containing 2% BSA and 15% prewashed canine red blood cells adjusted to pH 7.40 and oxygenated via a silastic tubing lung, ventilated with an atmosphere of 100% pure oxygen. A peristaltic pump was used as single passed perfusion system. Perfusions were adjusted to a flow rate of 15 ml/min. The animals were sacrificed by thoracotomy once perfusion was established, and the inferior vena cava was cannulated for collection of samples. The animals were placed in a temperature-controlled environment at 37°C. Assessment of liver viability was by macroscopic appearance, measurement of bile flow, oxygen consumption and portal vein pressure.

Experimental Protocol

After a 10 min perfusion-stabilization period, [U-^{14}C] sucrose (1.5×10^5 dpm) was injected into the liver with outlet samples collected via a fraction collector over 4 min. Two digoxin doses of 42 and 125 µg were infused within 1 min, and 38 outflow samples were collected up to 7 min after starting of infusion. All outflow samples were centrifuged, and aliquots (100 µL) of supernatant were taken for analysis.

Analytical Procedure

The [U-^{14}C]sucrose samples were taken for scintillation counting using a MINAXI beta TRICARB 4000 series liquid scintillation counter (Packard Instruments, Meriden, CT). For determination of digoxin concentration in outflow samples, a published LC/MS/MS method with online solid phase extraction (15) was optimized. One-hundred µl of the collected perfusate were transferred into a 1.5 ml Eppendorf tube, spiced with 10 µl 200 ng/ml clindamycin (internal standard), 200 µl 0.1 M $ZnSO_4$ and 500 µl acetonitrile and were vigorously vortexed. After centrifugation at 13,000 × *g* for 10 min at 4°C, aliquots of the upper phase were transferred to the autosampler vials for the online solid phase extraction sample analysis. The LC/MS/MS system consisted of three LC-10AT HPLC pumps (Shimadzu), an SCL-10A XL auto injector (Shimadzu), an SCL-10A VP system controller (Shimadzu) and an API 2000™ LC/MS/MS System (Applied Biosystems). Phenomenex online extraction column (C18, 10×2 mm) and Phenomenex gemimi (5 µm, C18, 50×2 mm) with Phenomenex guard column (5 µm, C18 4×3 mm) were used for online solid phase extraction and LC separation, respectively. Two different mobile phases were attached to the three different HPLC pumps: pump A and pump B (20 µM ammonium formate in Milli-Q Water) and pump C (90% acetonitrile; 5% methanol; 5% water). An optimized gradient chromatography was used for online solid phase extraction and chromatography separation. The retention times of digoxin and clindamycin (internal standard) are 4.9 min and 3.0 min, respectively. The base line of the blank perfusion solution was free of interference. The detector response of digoxin was linear over the range from 2 ng/ml to 5 µg/ml ($R^2>0.999$) and was prepared

daily with digoxin stock solution. The limit of quantification was 2 ng/ml. The intra-day and inter-day variability of digoxin were lower that 10%. After the analytical run, samples with concentration over 5.0 μg/ml were diluted with perfusion buffer solution and analyzed once again.

MODEL

We extended a liver model previously developed by Anissimov and Roberts (9), where the spatial heterogeneity in sinusoidal mixing is modeled by a chain of eight compartments (compartments 1 to 8 in Fig. 1). This model, which well described the impulse-response profile of the vascular marker, was already successfully validated in the linear case, where it led for palmitate to results comparable to those obtained with distributed models (9). To incorporate saturable uptake into the model, the uptake rate constant k_{in} was replaced by the Michaelis-Menten model (Model 1MM)

$$k_{in}(t) = \frac{V_{\max}}{K_M + C(t)} \tag{1}$$

where $C = C(t)$ is the compartmental drug concentration (suppressing the subscript i), and $V_{\max}$ and K_M, denote the maximal rate of digoxin uptake and apparent Michaelis constant (inverse affinity constant), respectively. Since the resulting parameter estimates were not consistent with those obtained previously (3), we also tested an alternative model assuming two saturable components (Model 2MM) :

$$k_{in}(t) = \frac{V_{\max 1}}{K_{M1} + C(t)} + \frac{V_{\max 2}}{K_{M2} + C(t)} \tag{2}$$

Alternatively, the second Michaelis-Menten term in Eq. 2 is replaced by a passive (nonsaturable) component with rate constant k_p (Model MMkp):

$$k_{in}(t) = \frac{V_{\max 1}}{K_{M1} + C(t)} + k_p \tag{3}$$

To account for saturable sinusoidal binding, a binding site was added in the vascular compartments where the bound drug concentration $C_b(t)$ is governed by the association and dissociation rates:

$$dC_b(t)/dt = k_{on}[R_{tot} - C_b(t)]C(t) - k_{off}C_b(t) \tag{4}$$

where again $C(t)$ is the free drug concentration in the vascular compartment (i.e., $C(t)$ and $C_b(t)$ stand for $C_i(t)$ and $C_{bi}(t)$, respectively, with $i = 1..8$), k_{on} and k_{off} denote the association and dissociation rate constants, respectively, and R_{tot} is the unknown concentration of available receptor sites. Sinusoidal binding is characterized by the dissociation constant $K_D = k_{off} / k_{on}$. The final structure of the model is shown in Fig. 1. The vascular volume V and four transfer constants between vascular compartments (two between 3 to 5 and two between 3 and 4, and 5 and 6) have to be estimated by fitting the eight-compartartment model to impulse-response outflow data of sucrose. Note that the rate constants between compartments 1 to 3 and 5 to 8 are determined by the vascular volume and flow rate Q. For details, please see (9).

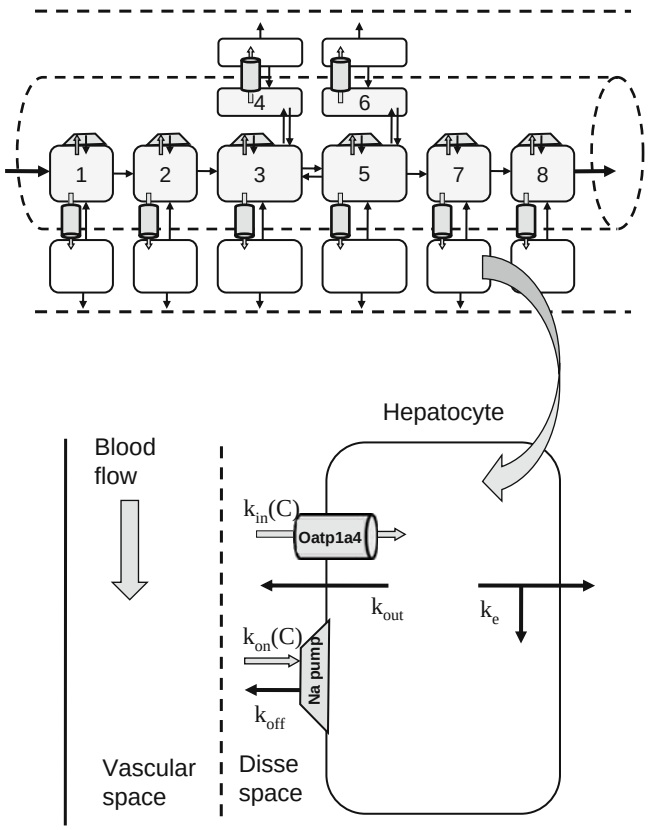

Fig. 1 Compartmental model to describe the sinusoidal concentration gradient (compartments 1 to 8) (9) extended by saturable sinusoidal binding (Na pump) and uptake (Oatp1a4) of digoxin. The parameters $k_{in}(C)$ and d $k_{on}(C)$ denote concentration-dependent uptake and binding, respectively, k_{out} is the efflux rate constant, k_{off} the dissociation rate constant, and k_e denotes the elimination rate constant (biliary excretion and metabolism). Note that the auxillary compartments 4 and 6 were introduced to improve the fit in the tail part of the outflow curve (9). (The Na pumps have been omitted in these compartments to simplify the graph.) Like the other compartments, they have no direct physiological meaning.

DATA ANALYSIS

First, the differential equations corresponding to the eight-compartment model of vascular mixing were fitted to the [^{14}C] sucrose outflow data to estimate the parameters T, k_b, a, b of the model #7 in (9). (These parameters determine extracellular sucrose space, V.) The catheter effect was

corrected by a lag time, t_{lag}. These 5 parameters were estimated for each liver and then fixed in fitting the digoxin outflow data using a model (Fig. 1) represented by a system of 22 differential equations. In doing so, the digoxin-specific parameters V_{maxi}, K_{Mi}, k_{on}, k_{off}, R_{tot} and k_e are estimated (using the reparameterization (V_{maxi} /K_{Mi}) to improve identifiability). The digoxin data were analyzed by a population approach with maximum likelihood estimation via the EM algorithm (16,17) implemented in the software ADAPT 5 (10). The MLEM program provides estimates of the population mean and inter-subject variability as well as of the individual subject parameters (conditional means). We assumed log-normally distributed model parameters and that the measurement error has a standard deviation that is a linear function of the measured quantity.

Because the estimation of parameters of a system containing three saturable processes is an ill-posed problem, prior information on the binding and transport processes is necessary in order to reduce the large range of likely solutions. While initial guesses of the Michaelis-Menten parameters for the high affinity uptake process are available from the literature and previous experiments (3), quantitative information on binding of digoxin to hepatic Na,K-ATPase is scarce. Thus, we used values of k_{on}, k_{off} and R_{tot} from various sources and compared the resulting fits. The initial values for parameter inter-subject variability were set at 40% of their mean values. Note that the results of the MLEM fit are dependent on this prior probability distribution rather than the starting values. Due to the extremely low digoxin extraction of less than 5% in rat liver, prior information on the elimination rate constant k_e taken from the literature (7) had to be incorporated. After analyzing the present data, the new model was also applied to our previously published data (3).

RESULTS

Fig. 2 shows that the vascular mixing model (compartments 1–8 in Fig. 1) well described the transit time density (outflow curve) of the extracellular marker sucrose. The estimated parameters (see model # 7 in (9)) were found to be $T=0.11\pm0.02$ min, $k_b=22.7\pm7.4$ min^{-1}, $a=2.3\pm1.1$ min^{-1}, $b=4.7\pm1.6$ min^{-1} and $t_{lag}=0.038\pm0.006$ min. The resulting extracellular volume (Eq. A18 in (9)) was $V=2.35\pm0.47$ ml.

In fitting the digoxin data using only one saturable uptake process (Model 1MM, Eq. 1), it became obvious that V_{max} and K_M were about 1,000-fold higher than those obtained previously with lower doses (15 to 45 μg instead of 42 and 125 μg) (3), while the ratio V_{max} /K_M remained nearly unchanged. In order to reveal this inconsistency, Model 2MM (Eq. 2) was fitted to the data, using the

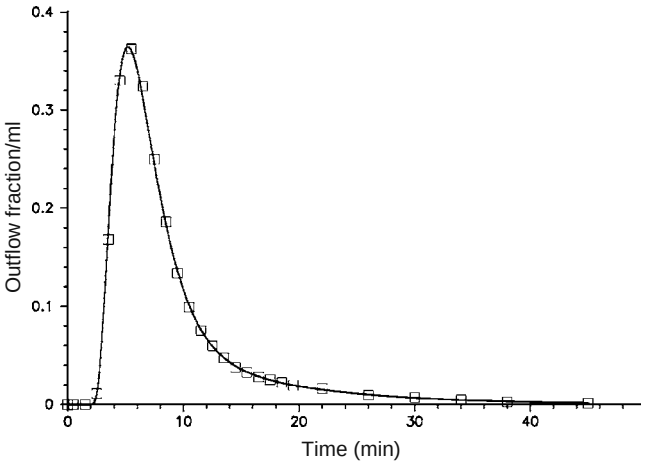

Fig. 2 Typical fit of [^{14}C]-sucrose outflow profile obtained with the 8-compartment model (Fig. 1).

estimates obtained with lower doses (3) as initial values for V_{max1} and K_{M1}. The initial guesses for the binding parameters are based on the K_D and R_{tot} values of ouabain binding to Na,K-ATPase observed in rat liver (18), assuming $k_{off}=0.7$ min^{-1}(19). The observed and model-predicted digoxin outflow curve is depicted in Fig. 3A for one liver as an illustrative example. The overall quality of fit is demonstrated in Fig. 3B, showing the correlation of the predicted *versus* the measured concentration for all livers. Parameter estimates with interindividual variability in parentheses are listed in Table I. The results reveal the existence of high-affinity/low-capacity and a low-affinity/high-capacity sinusoidal uptake system characterized by $K_{M1}=0.24$ μg/ml, $V_{max1}=16.1$ μg ml^{-1} min^{-1} and $K_{M2}=332$ μg/ml $V_{max2}=17{,}800$ μg ml^{-1} min^{-1}, respectively. It is very important to note that it was not possible to obtain a good fit and reasonable parameter estimates using the previous well-mixed model (3) (see below). Without incorporating saturable sinusoidal binding, systematic deviations were observed in peak region of the curve (first 2 min). To demonstrate the consistency of the present results with those reported previously for lower doses using a well-mixed model, the outflow data obtained after three consecutive digoxin doses of 15, 30 and 45 μg (3) were fitted using the new model and the population approach (after estimating the parameters of the concomitant sucrose outflow curves). Because information on the low-affinity/high-capacity uptake process is limited in these experiments, the present parameter estimates were used as priors to set the ranges for K_{M2} and V_{max2}. Fig. 4A and B show that the new model fits also the data in the lower dose range very well; the parameter estimates are consistent with those obtained in the high dose experiments. A fit of the same quality was achieved assuming only one saturable component (Model 1MM). This indicates the predominance of the

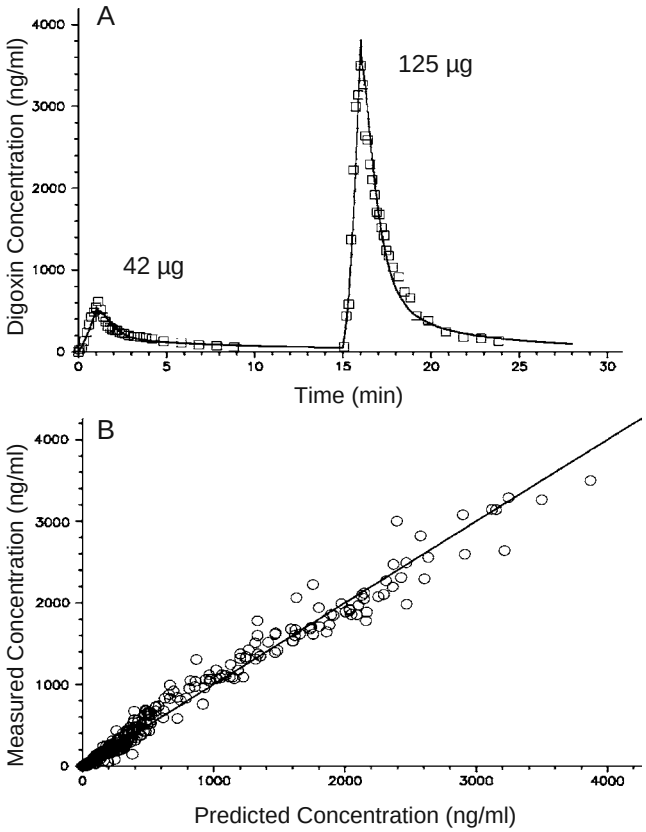

Fig. 3 Fit of high-dose digoxin outflow data in one liver using Model 2MM (**A**) and goodness-of-fit plot, showing the observed concentration *versus* individual predicted concentration (**B**). The *solid line* represents the line of identity.

high-affinity uptake system at doses below 50 µg. In contrast to the present high dose experiments, the data obtained with lower doses could be fitted assuming a well-mixed vascular space and neglecting the effect of digoxin binding (3). The homogeneity model slightly underestimated K_M. Likewise, the neglect of digoxin binding has only a small effect on the K_M and V_{max} estimates in the 15 to 45 µg dose range. A crucial question of model selection was whether Model MMkp, where the low affinity uptake component is replaced by a passive process (Eq. 3), would fit the data equally well as Model 2MM. Although Model MMkp describes the high dose data reasonably well and the V_{max1} and K_{M1} estimates are consistent with those of the 2MM model (Tab. I), it does not fit the 15 to 45 µg dose data, where a fit is only obtained for $k_p \approx 0$.

DISCUSSION

Although recent advances in molecular biology have identified hepatic uptake transporters, little is known about their functional properties *in situ* (in terms of Michaelis-Menten parameters). One of the reasons may be that the construction of mathematical models for nonlinear pharmacokinetic systems is challenging, and the estimation of model parameters is a difficult task. While the simple liver model of digoxin uptake that was based on the approximation of (i) a well-mixed vascular space, (ii) only one uptake system and (iii) neglect of specific binding fitted the lower dose digoxin data reasonable well (3), it failed in the

Table I Parameter Estimates (MLEM) From Fitting of Digoxin Outflow Concentration Data Following Two Consecutive Doses of 42 and 125 µg in the Perfused Rat Liver Using Sucrose as Reference for the Sinusoidal Space ($n = 5$)

Model		2MM		MMkp	
AIC		−216		−182	
Estimated parameters		Average value	Inter-individual variability (%)	Average value	Inter-individual variability (%)
Uptake and elimination					
V_{max1} /K_{M1}	(min^{-1})	66.1	82	84.4	44
K_{M1}	(µg/ml)	0.243	13	0.24	6
V_{max2} /K_{M2}	(min^{-1})	53.6	25	–	–
K_{M2}	(µg/ml)	332	40	–	–
k_{out}	(min^{-1})	5.69	6	4.86	21
k_e	(min^{-1})	0.022	163	0.027	75
k_p	(min^{-1})	–	–	47.3	28
Binding					
k_{on}	(ml μg^{-1} min^{-1})	0.00053	18	0.0005	32
k_{off}	(min^{-1})	0.121	52	0.109	34
R_{tot}	(µg/ml)	20.7	40	20.4	47
Derived parameters					
V_{max1}	(µg ml^{-1} min^{-1})	16.1	47	20.2	45
V_{max2}	(µg ml^{-1} min^{-1})	17800	83	–	–
K_D	(µg/ml)	0.228	55	0.216	46

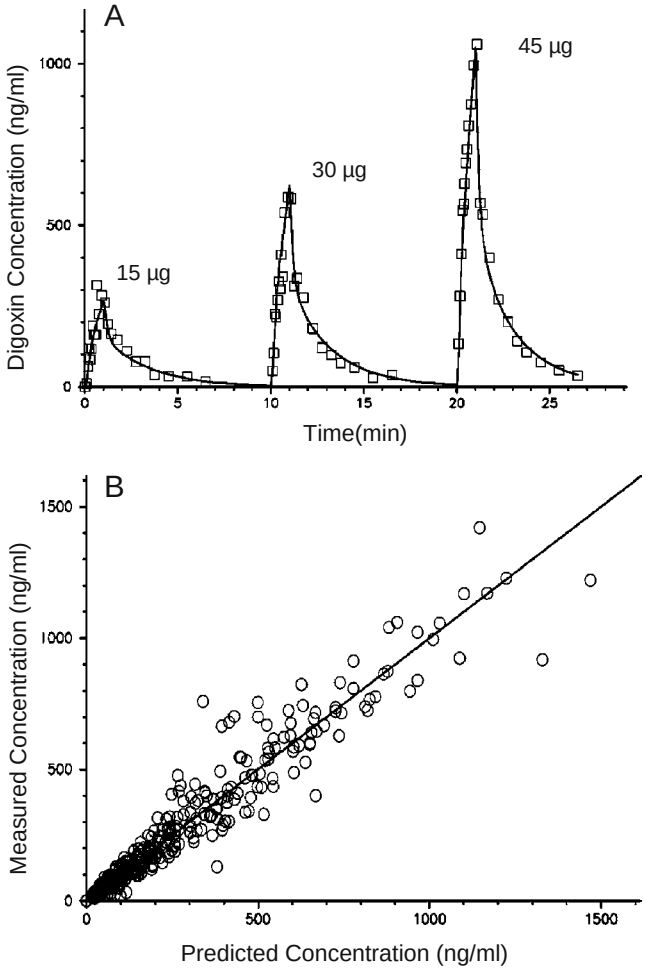

Fig. 4 Fit of low-dose digoxin outflow data (3) in one liver using Model 2MM (**A**) and goodness-of-fit plot, showing the observed concentration *versus* individual predicted concentration (**B**). The *solid line* represents the line of identity.

high dose range (where maximum outflow concentration was about 3-fold higher). The objective of this study was to develop a more realistic model that fits the digoxin data over the whole dose range. The essential improvements are the use of a heterogeneous (semi-distributed) liver model and incorporation of saturable binding.

The results suggest that digoxin uptake into the rat liver is apparently mediated by two kinds of transporters. At low extracellular concentration, digoxin was taken up through a saturable high affinity system (K_{M1}=0.24 µg/ml) with low capacity (V_{max1}=61.1 µg ml^{-1} min^{-1}), while at higher concentration digoxin uptake proceeds essentially via low affinity transporter (K_{M2}=332 µg/ml) with high capacity (V_{max2}=17,800 µg ml^{-1} min^{-1}). Our estimate of K_{M1} is in accordance with the high affinity of digoxin for Oatp1a4 (20,21), but we are not aware of any published data on a low affinity transporter for digoxin uptake. One reason may be the lack of data in the higher dose range, especially in the liver *in situ*, or that low affinity component was mistakenly regarded as passive diffusion. Furthermore, previous approaches did not take the effect of digoxin binding to hepatic Na,K-ATPase into account.

While the binding kinetics of digoxin to cardiac Na,K-ATPase have been studied in the isolated perfused rat heart (19,22), such information is lacking for the liver. The distribution of Na pumps in the rat liver is largely understood (4,5), but there is substantially less quantitative data available on binding affinity and expression. Our estimates of the concentration of saturable sinusoidal binding sites (R_{tot}=20.7 µg/ml) are in the same order of magnitude, but the dissociation constant (K_D=0.23 µg/ml) is lower than the values observed for ouabain in the rat heart (R_{tot}=1 µg/ml and K_D=7 µg/ml). However, our estimate of K_D is similar to that of 0.33 µg/ml reported for ouabain in the guinea pig liver (23). The concentration of binding sites R_{tot} estimated here by kinetic modeling is not much different from that obtained by antibody binding in the rat liver (24). Compared with our results for digoxin binding to the low affinity binding site (α_1-isoform of Na,K-ATPase) in the perfused rat heart (18), the K_D values estimated here in the perfused liver are much lower. If we used the rat heart data as initial guesses, we obtained similar estimates but at the cost of a worse fit to the data. Note that incorporation of saturable binding kinetics was necessary to fit the high dose data; that this effect was not detected in fitting the 15 to 45 µg dose data (3) was probably due to linear binding and the assumption of well-mixed distribution (which covers binding kinetics).

This study, for the first time, provides direct kinetic evidence for a high-affinity, low-capacity and low-affinity, high-capacity uptake system of digoxin in the sinusoidal membrane. The existence of two apparent functional sites on OATP transporter was first shown by Tamai *et al.* (12), and a functional role of multiple binding sites in rat Oatp1a4 was suggested by Sugiyama *et al.* (25). Apparently, the high-affinity, low-capacity Oatp/OATP system dominates at physiological (and therapeutic) substrate concentrations, and the very high-affinity uptake of digoxin is a unique property of Oatp1a4. Much higher digoxin concentrations are necessary to reveal the low-affinity, high-capacity uptake system, while the high-affinity component is readily saturable. K_M ratios of 100 (12) and a low-affinity K_M in the millimolar range (26,27) have been reported for OATPs and Oatp1, respectively. Note that due to the sinusoidal gradient, outflow concentration does not represent digoxin concentration at the site of transporters (except in compartment 8); the concentration in compartment 2 (Fig. 1), for example, is 20-fold higher. Although this concentration is about the same order of magnitude as K_{M2}, it is still lower, and this may affect the reliability of the K_{M2} estimate.

One inherent limitation of the present approach is that the model is not uniquely identifiable due to the complexity of the nonlinear system. Thus, a critical question is whether indeed the assumption of a nonsaturable component of hepatic digoxin uptake (7) indicates that the transporter has a very high K_M value, or whether the converse is true. We have tested this question by replacing the high affinity by a nonsaturable component (Model MMkp instead of Model 2MM). Although the fit was equally good, the estimates of K_{M1}, V_{max1} and k_p of the high and low dose experiments were not consistent. That an apparent nonsaturable component observed at low concentrations may indicate the contribution of a low affinity uptake process was previously suggested for other transporters (28,29). The results obtained with simpler models are also shown for comparison (Fig. 5). That the introduction of saturable sinusoidal binding considerably improved the fit is obvious from the reduction in *AIC* from −36 to −216 (Fig. 5A). The main reason for rejection of the model that is based on a well-mixed vascular space (3) is not the significantly worse fit but the unrealistic estimates of K_M and V_{max} that are 2- fold and 50-fold higher, respectively, than those obtained in experiments with lower doses (3) (Fig. 5B). The effect of a change in the concentration of sinusoidal binding sites on digoxin outflow curves has been simulated in Fig. 6. Our results provide at least some evidence that saturable binding may play a role for high digoxin doses; specially designed experiments are necessary to resolve this question. As discussed in our previous paper, elimination had a negligible effect on the outflow curve due to the low hepatic extraction of digoxin, and the k_e estimate is mainly determined by the prior.

In using prior information to constrain the parameters, an important model selection criterion was the condition that the model should fit the data over the whole dose range. Although simpler models fit either the lower or higher dose data, the resulting parameter estimates were not consistent. However, the present results show that the simplicity of a well-mixed sinusoidal space without saturable binding may be justified in the low dose range, where it fitted the data (but probably on the cost of an overestimation of K_{M1}) (3). That it failed to fit the high dose data may indicate that with increasing dose the concentration gradient along the liver may play a greater role in determining drug uptake. In contrast to homogeneous representations, the present model can also account for the zonal heterogeneity of the liver. However, for our single-pass data, incorporation of zonal differences in Michaelis-Menten uptake parameters of digoxin (7) did not significantly improve the fit.

Being fully aware of the limitations inherent in the use of complex nonlinear models, we only infer that the selected model (Fig. 1) best explains our high dose digoxin data. Since the results are based on the incorporation of prior information (e.g., the high-affinity uptake system could not be identified on the basis of the high dose data alone), the approach resembles in this respect the method of forward modeling (simulation) where the emphasis is on

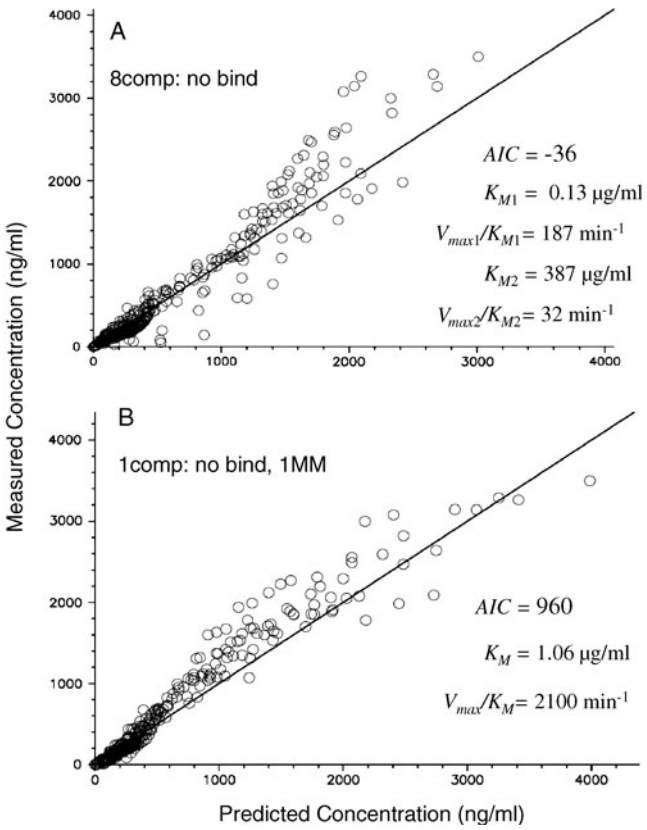

Fig. 5 Effect of model simplification: Model 2MM without binding (Fig. 1 without Na pumps) (**A**) and the vascular well-mixed 1MM model without binding (**B**).

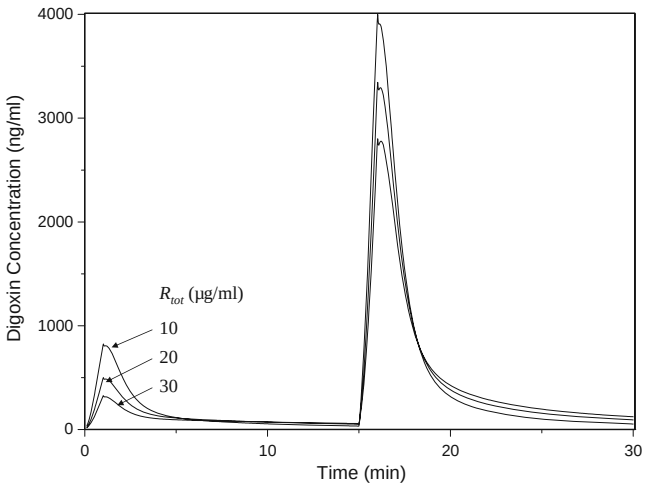

Fig. 6 Simulation of the effect of changes in Na pump concentration (R_{tot} = 10, 20 and 30 μg/ml) on digoxin outflow curve (using mean parameters of the 2MM Model, Table I).

understanding through modeling. While simpler models may be sufficient in the lower dose range of saturable kinetics, it cannot be excluded that the assumption of a well-mixed vascular compartment leads to biased parameter estimates (as for linear kinetics), since hepatic pharmacokinetics is a distributed-in-space process. The semi-distributed model may be a useful alternative in case of nonlinear systems,

In summary, the following model improvements made a fit of the high dose digoxin data possible: 1) use of a semi-distributed liver model, 2) incorporation of saturable sinusoidal binding, and 3) assumption of a high-affinity, low-capacity and low-affinity, high-capacity uptake system. Future studies using high substrate concentrations are needed to support the hypothesis of biphasic uptake kinetics of digoxin. The semi-distributed liver model with saturable uptake could be useful to elucidate the role of hepatic transporters in the isolated perfused rat liver using sucrose as a reference for the sinusoidal space. *In silico* liver models play an important role in translational research, e.g. the scale-up of *in vitro* data to the whole organ (30,31).

ACKNOWLEDGEMENTS

We thank Y. Anissimov for discussions and advice. This work was supported by grants from the Australian National Health & Medical Research Council (569710 and 401505) and the Deutsche Forschungsgemeinschaft, Bonn, Germany (WE 2190/5-1).

REFERENCES

1. Benet LZ. The drug transporter-metabolism alliance: uncovering and defining the interplay. Mol Pharm. 2009;6(6):1631–43.
2. Li P, Wang GJ, Robertson TA, Roberts MS. Liver transporters in hepatic drug disposition: an update. Curr Drug Metab. 2009;10:482–98.
3. Weiss M, Hung DY, Poenicke K, Roberts MS. Kinetic analysis of saturable uptake of digoxin and its inhibition by rifampicin. Eur J Pharm Sci. 2008;34:345–50.
4. Simon FR, Leffert HL, Ellisman M, Iwahashi M, Deerinck T, Fortune J, *et al.* Hepatic Na(+), K(+)-ATPase enzyme activity correlates with polarised beta-subunit expression. Am J Physiol. 1995;269:C69–84.
5. Benkoël L, Benoliel AM, Brisse J, Sastre B, Bongrand P, Chamlian A. Immunocytochemical study of Na+K(+)-ATPase alpha and beta subunits in human and rat normal hepatocytes using confocal microscopy. Cell Mol Biol. 1995;41:499–504.
6. Lau YY, Wu CY, Okochi H, Benet LZ. *Ex situ* inhibition of hepatic uptake and efflux significantly changes metabolism: hepatic enzyme-transporter interplay. J Pharmacol Exp Ther. 2004;308:1040–5.
7. Liu L, Mak E, Tirona RG, Tan E, Novikoff PM, Wang P, *et al.* Vascular binding, blood flow, transporter, and enzyme interactions on the processing of digoxin in rat liver. J Pharmacol Exp Ther. 2005;315:433–48.
8. Rubin GM, Tozer TN. Hepatic binding and Michaelis-Menten metabolism of drugs. J Pharm Sci. 1986;75:660–3.
9. Anissimov YG, Roberts MS. A compartmental model of hepatic disposition kinetics: 1. Model development and application to linear kinetics. J Pharmacokinet Pharmacodyn. 2002;29:131–56.
10. D'Argenio DZ, Schumitzky A, Wang X. ADAPT 5 user's guide: pharmacokinetic /pharmacodynamic systems analysis software. Los Angeles: Biomedical Simulations Resource; 2009.
11. Krudys KM, Kahn SE, Vicini P. Population approaches to estimate minimal model indexes of insulin sensitivityand glucose effectiveness using full and reduced sampling schedules. Am J Physiol Endocrinol Metab. 2006;291:E716–23.
12. Tamai I, Nozawa T, Koshida M, Nezu J, Sai Y, Tsuji A. Functional characterization of human organic anion transporting polypeptide B (OATP-B) in comparison with liver-specific OATP-C. Pharm Res. 2001;18:1262–9.
13. Westholm DE, Salo DR, Viken KJ, Rumbley JN, Anderson GW. The blood-brain barrier thyroxine transporter organic anion-transporting polypeptide 1c1 displays atypical transport kinetics. Endocrinology 2009;150:5153–62.
14. Cheung K, Hickman PE, Potter JM, Walker N, Jericho M, Haslam R, *et al.* An optimised model for rat liver perfusion studies. J Surg Res. 1996;66:81–9.
15. Yao M, Zhang H, Chong S, Zhu M, Morrison RA. A rapid and sensitive LC/MS/MS assay for quantitative determination of digoxin in rat plasma. J Pharm Biomed Anal. 2003;32:1189–97.
16. Schumitzky A. EM Algorithms and two stage methods in pharmacokinetic population analysis. In: D'Argenio DZ, editor. Advanced methods of pharmacokinetic and pharmacodynamic systems analysis, vol. II. New York: Plenum; 1995.
17. Walker S. An EM algorithm for nonlinear random effects models. Biometrics 1996;52:934–44.
18. Lin MH, Akera T. Increased (Na+, K+)-ATPase concentrations in various tissues of rats caused by thyroid hormone treatment. J Biol Chem. 1978;253:723–6.
19. Weiss M, Baek M, Kang W. Systems analysis of digoxin kinetics and inotropic response in rat heart: effects of calcium and KB-R7943. Am J Physiol Heart Circ Physiol. 2004;287:H1857–67.
20. Noé B, Hagenbuch B, Stieger B, Meier PJ. Isolation of a multispecific organic anion and cardiac glycoside transporter from rat brain. Proc Natl Acad Sci USA. 1997;94:10346–50.
21. Cattori V, van Montfoort JE, Stieger B, Landmann L, Meijer DK, Winterhalter KH, *et al.* Localization of organic anion transporting polypeptide 4 (Oatp4) in rat liver and comparison of its substrate specificity with Oatp1, Oatp2 and Oatp3. Pflugers Arch. 2001;443:188–95.
22. Kang W, Weiss M. Digoxin uptake, receptor heterogeneity, and inotropic response in the isolated rat heart: a comprehensive kinetic model. J Pharmacol Exp Ther. 2002;302:577–83.
23. Harashima H, Mamiya M, Yamazaki M, Sawada Y, Iga T, Hanano M, *et al.* Kinetic modeling of ouabain tissue distribution based on slow and saturable binding to Na, K-ATPase. Pharm Res. 1992;9:1607–11.
24. Schenk DB, Hubert JJ, Leffert HL. Use of a monoclonal antibody to quantify (Na+, K+)-ATPase activity and sites in normal and regenerating rat liver. J Biol Chem. 1984;259:14941–51.
25. Sugiyama D, Kusuhara H, Shitara Y, Abe T, Sugiyama Y. Effect of 17 beta-estradiol-D-17 beta-glucuronide on the rat organic anion transporting polypeptide 2-mediated transport differs depending on substrates. Drug Metab Dispos. 2002;30:220–3.

26. van Montfoort JE, Stieger B, Meijer DK, Weinmann HJ, Meier PJ, Fattinger KE. Hepatic uptake of the magnetic resonance imaging contrast agent gadoxetate by the organic anion transporting polypeptide Oatp1. J Pharmacol Exp Ther. 1999;290:153–7.
27. Nakakariya M, Shimada T, Irokawa M, Koibuchi H, Iwanaga T, Yabuuchi H, *et al*. Predominant contribution of rat organic anion transporting polypeptide-2 (Oatp2)to hepatic uptake of beta-lactam antibiotics. Pharm Res. 2008;25:578–85.
28. Chen J, Zhu Y, Hu M. Mechanisms and kinetics of uptake and efflux of L-methionine in an intestinal epithelial model (Caco-2). J Nutr. 1994;124:1907–16.
29. Bettendorff L, Wins P. Mechanism of thiamine transport in neuroblastoma cells. Inhibition of a high affinity carrier by sodium channel activators and dependence of thiamine uptake on membrane potential and intracellular ATP. J Biol Chem. 1994;269:14379–85.
30. Ierapetritou MG, Georgopoulos PG, Roth CM, Androulakis IP. Tissue-level modeling of xenobiotic metabolism in liver: an emerging tool for enabling clinical translational research. Clin Transl Sci. 2009;2:228–37.
31. Rostami-Hodjegan A, Tucker GT. Simulation and prediction of *in vivo* drug metabolism in human populations from *in vitro* data. Nat Rev Drug Discov. 2007;6:140–8.